An adapted RANS RSM wall function for building external convection

Lucie Merlier, Frederic Kuznik, Gilles Rusaouen, Julien Hans

▶ **To cite this version:**

Lucie Merlier, Frederic Kuznik, Gilles Rusaouen, Julien Hans. An adapted RANS RSM wall function for building external convection. Building and Environment, 2015, 94 (2), pp.654-664. 10.1016/j.buildenv.2015.10.010 . hal-01287528

HAL Id: hal-01287528
https://hal.science/hal-01287528

Submitted on 24 May 2023

HAL is a multi-disciplinary open access archive for the deposit and dissemination of scientific research documents, whether they are published or not. The documents may come from teaching and research institutions in France or abroad, or from public or private research centers.

L'archive ouverte pluridisciplinaire **HAL**, est destinée au dépôt et à la diffusion de documents scientifiques de niveau recherche, publiés ou non, émanant des établissements d'enseignement et de recherche français ou étrangers, des laboratoires publics ou privés.

Accepted Manuscript

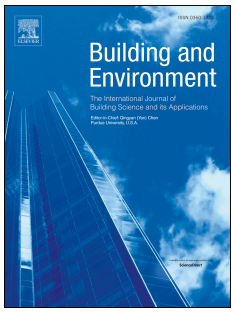

An adapted steady RANS RSM wall-function for building external convection

Lucie Merlier, Frédéric Kuznik, Gilles Rusaouën, Julien Hans

PII: S0360-1323(15)30149-9

DOI: 10.1016/j.buildenv.2015.10.010

Reference: BAE 4278

To appear in: *Building and Environment*

Received Date: 20 August 2015

Revised Date: 3 October 2015

Accepted Date: 17 October 2015

Please cite this article as: Merlier L, Kuznik F, Rusaouën G, Hans J, An adapted steady RANS RSM wall-function for building external convection, *Building and Environment* (2015), doi: 10.1016/j.buildenv.2015.10.010.

This is a PDF file of an unedited manuscript that has been accepted for publication. As a service to our customers we are providing this early version of the manuscript. The manuscript will undergo copyediting, typesetting, and review of the resulting proof before it is published in its final form. Please note that during the production process errors may be discovered which could affect the content, and all legal disclaimers that apply to the journal pertain.

ACCEPTED MANUSCRIPT

An adapted steady RANS RSM wall-function for building external convection

Lucie Merlier[a,b,*], Frédéric Kuznik[a], Gilles Rusaouën[a], Julien Hans[b]

[a] *CETHIL, UMR5008, Université de Lyon, CNRS, INSA-Lyon, Univ. Lyon 1, F-69621, Villeurbanne, France*
[b] *CSTB, Direction Energie Environnement, F-38400, Saint Martin d'Hères, France*

Abstract

Computational Fluid Dynamics (CFD) can improve usual estimates of building external convective heat transfer coefficients ($h_{c,w}$) by accounting for the geometry of constructions, the aerodynamic field around them, the nature of convection and providing high resolution data. However, the limitations of usual mass flow descriptions and near wall treatments make the accurate prediction of $h_{c,w}$ challenging. Hence, this paper evaluates the ability of steady RANS Reynolds Stress (RSM) and k-ε realizable models to predict $h_{c,w}$ in case of isolated cubical obstacles. The accuracy of usual CFD methods and turbulence models, as well as fine grid near wall models and usual temperature wall functions (TWFs) are examined by comparison with experimental and detailed numerical data.

When used with a low Reynolds number model (LRNM), both turbulence models accurately predict $h_{c,w}$ on the front and rear faces of the obstacle. However, they show different behaviors on the other faces and highlight issues related to the dynamic behavior of real flows. Moreover, $h_{c,w}$ predictions obtained using standard TWFs substantially deviate from the validated LRNM results. Therefore, a customized TWF suited for use with the RSM and forced convection problems is proposed by extending studies of Defraeye et al. (An adjusted temperature wall function for turbulent forced convective heat transfer for bluff bodies in the atmospheric boundary layer; Building and Environment, 2011, 46, 2130-2141). Customized TWFs substantially improve WF-based hcw predictions with respect to LRNM results while keeping their cost effectiveness, and provides satisfactory results even for high z^*.

*Corresponding author. Tel.: +33-472-437-483; Fax: +33-472-438-522
Email address: lucie.merlier@insa-lyon.fr (Lucie Merlier)

ACCEPTED MANUSCRIPT

Highlights

- Steady RANS hcw predictions are studied on the front and rear faces of cubes
- RkE and RSM -LRNM models are accurate but standard TWF overestimate hcw
- An adapted TWF for the RSM is proposed based on the methodology of (Defraeye, 2011)
- Customized TWFs perform satisfactorily for high z*

Keywords

- External convective heat transfer coefficient
- Steady RANS method
- 1st and 2nd order turbulence models
- Low Reynolds number modeling
- Temperature wall function

ACCEPTED MANUSCRIPT

ACCEPTED MANUSCRIPT

Nomenclature

Main Abbreviations		
CFD	Computational Fluid Dynamics	
LBM	Lattice Boltzmann Method	
LES	Large Eddy Simulation	
LRNM	Low Reynolds number modeling	
RANS	Reynolds Averaged Navier–Stokes	
Rk-ε	Realizable k-ε	
RSM	Reynolds Stress Model	
(C)(T)WF	(Customized) (Temperature) Wall Function	
Main Symbols and constants		
ρ	Gas density	$[\mathrm{kg} \cdot \mathrm{m}^{-3}]$
Cp	Specific heat	$[\mathrm{J} \cdot \mathrm{kg}^{-1} \cdot \mathrm{K}^{-1}]$
C_μ	Model constant	$[-]$
h	Surface heat transfer coefficient	$[\mathrm{W} \cdot \mathrm{m}^{-2} \cdot \mathrm{K}^{-1}]$
k	Turbulent kinetic energy	$[\mathrm{m}^2 \cdot \mathrm{s}^{-2}]$
q	Density of heat transfer	$[\mathrm{W} \cdot \mathrm{m}^{-2}]$
T	Temperature	[K]
T^*	Dimensionless temperature	$[-]$
U	Streamwise velocity	$[\mathrm{m} \cdot \mathrm{s}^{-1}]$
z^*	Dimensionless wall unit	$[-]$
z_0	Aerodynamic roughness length	[m]
Subscripts		
c	convective	
p	first cell	
ref	reference	
t	turbulent	
T	thermal	
w	wall	
Dimensionless numbers		
Pr	Prandtl number	
Re	Reynolds number	
Ri	Richardson number	

ACCEPTED MANUSCRIPT

Introduction

The accurate knowledge of building interior and exterior convective heat transfers is required to properly evaluate the building thermal and energy behavior [1, 2, 3, 4, 5, 6]. Only considering external convective heat transfers, they are also important to study the performance of energy systems [7] including the convective cooling of solar panels, the drying behavior of surfaces [8] or the turbulent thermal transfers in cities, which influence the urban heat island [9, 10].

Convective heat transfers depend on different parameters related to the properties of the fluid, flow and surface. Considering air and a basic boundary layer configuration over a flat plate, they directly depend on the flow velocity and turbulence as well as on the surface roughness. On the contrary, sharp edged obstacles generally involve complex separated flows. As a consequence, convective heat transfers are greatly determined by the different properties of the flow structures that develop next to the obstacles [11, 12, 13]. In particular, heat entrapment into the recirculation phenomena decreases heat transfers whereas high wind speeds and temperature differences between the fluid and the wall improve heat transfers in flow impinging regions. Similarly, the intermittent flow reattachment on the building surfaces improves convective heat transfers. Therefore, convective heat transfers distribution around bluff bodies such as buildings can completely differ from those developing over flat plates.

According to Ref. [14], existing correlations linking external convective heat transfer coefficient ($h_{c,w}$) with a reference wind speed and that are applicable for building outer walls are either based on reduced-scale experiments undertaken for bluff bodies located in a turbulent boundary layer [13, 15], full-scale measurements taken on building facades [16, 17] or computational fluid dynamics (CFD) modeling [3, 18, 19]. Nonetheless, according to [7] and [20], the different models commonly used in building thermal engineering and building energy simulation programs to compute building external convective heat transfers are generally derived from reduced-scale or full-

ACCEPTED MANUSCRIPT

scale experimental studies, and numerous and diverse models are reported. The fact that reduced-scale models often involve flat plates casts doubts on their applicability for building physics problems. Correlations derived from field measurements seem more suitable but their applicability is often limited as they correspond to specific configurations and experimental conditions. Therefore, further detailed experimental and computational studies are necessary to better understand the building energy behavior.

Compared to full-scale and wind-tunnel studies, CFD approaches can provide high resolution information and take into account most of the factors that influence $h_{c,w}$, including the different features of the approach flow, the effective dimensions, geometry and thermal properties of the built environment or the different natures of convection. However, usual CFD approaches have to deal with their intrinsic drawbacks due to their mathematical and physical assumptions [21, 22]. In particular, commonplace steady RANS methods cannot reproduce the intermittent flow behavior and turbulence models consider differently the effects of turbulence on the mean flow. Furthermore, $h_{c,w}$ predictions also greatly depend on the near wall treatment as, in addition to turbulent transport processes in the general mass flow, flow thermal features strongly vary in the wall viscous and buffer layers [23, 24]. Therefore, modeling accurately building external $h_{c,w}$ is even more complicated than it is for building aerodynamics alone, and find an appropriate couple of physical model and model resolution is challenging. Hence, considering isolated cubical case studies, this paper examines and discusses the accuracy of $h_{c,w}$ predictions obtained using (i) a steady RANS approach while dealing with strongly intermittent convective processes; (ii) first or second turbulence models (the k-ε realizable (Rk-ε) or Reynolds stress (RSM) models); and (iii) fine grid near wall models (LRNM) or wall functions (WF). A customized temperature wall-function (CTWF) suitable for use with the RSM and building physics problems is then proposed, extending the methodology proposed by [25].

To address these different issues, this paper is organized as follows. Sec. 1

ACCEPTED MANUSCRIPT

presents the modeling bases. Sec. 2 examines the accuracy of the LRNM model with respect to experimental data and analyzes the performance of implementing a steady RANS approach together with the Rk-ε or RSM models in predicting $h_{c,w}$ over an isolated cube. Then, Sec. 3 discusses deviations in $h_{c,w}$ predictions observed when using a standard TWF instead of the LRNM. Sec. 4 presents improvements of usual TWFs, and proposes a CTWF suitable for use with the RSM. Finally, Sec. 5 synthesizes the different results and methodological challenges highlighted trough the study and opens perspectives.

Note that this paper only focuses on convective heat transfers predictions. The validation of the different aerodynamic models used in the following can be found in Ref. [6, 26], in which the predicted flow fields around an isolated rectangular block immersed in a turbulent boundary layer are examined with respect to detailed wind-tunnel measurements of the CEDVAL [27, 28]. Predictions obtained using the steady RANS Rk-ε and RSM were found satisfactory and comparable next to the front and rear faces of the obstacle in case of a smooth floor.

1. Assessing building external convective heat transfer coefficients using CFD

Convective heat transfer at building external facade is generally expressed using a coefficient $h_{c,w}$, as follows:

$$h_{c,w} = \frac{q_{c,w}}{T_w - T_{ref}} \tag{1}$$

Uisng CFD, two main methods can be used to simulate the effects of a wall on the flow [29]. They differ by the complexity of the physical model and the grid resolution required. The more detailed approach is the LRNM. This method applies for $z^* \approx 1$ as it solves the whole boundary layer, including the laminar region. By contrast WFs require the first node to be located in the fully turbulent region of the boundary layer, i.e. $50 \leq z^* \leq 500$. WFs bridge in a single cell the viscosity affected region of the boundary layer and

ACCEPTED MANUSCRIPT

usually model near wall flow behavior using logarithmic laws. It is important to mention that usual WFs were derived from wall attached near equilibrium flows, which do not correspond to non equilibrium or separated flows [30]. Furthermore, the logarithmic formulation for temperature is even less widely valid than that for the momentum [24]. These reasons certainly explain, at least partly, why many studies including [23, 31] and [32] highlight the superiority of implementing LRNM or two layer models rather than WFs in predicting flow fields or/and convective heat transfers, although fine grid approaches are less cost effective and often reduce the simulation convergence rates. However, as opposed to fundamental CFD studies, using WFs is generally the only option when dealing with building physics problems because of the very different scales characterizing constructions and thermal boundary layers.

In the commercial CFD software Ansys Fluent [33], LRNM-based simulations can be performed using the so called "enhanced wall treatment" (EWT). This model can evolve from a LRNM approach to a enhanced WF formulation as z^* increases. For $z^* \approx 1$ this model behaves as a two layer zonal model. The viscosity affected region is solved using the one equation of Wolfshtein [34]. For $z^* \approx 1$, the dimensionless temperature (T^*) is computed as follows:

$$T^*_{lam} = Pr \left(z^+ \left(1 + \frac{\alpha}{2} z^+ \right) + \frac{\rho u^*}{2q} u^2 \right) \tag{2}$$

Considering incompressible flows and smooth walls, standard TWFs compute T^* as a linear or logarithmic function of z^* depending on the thermal sub-layer thickness z^*_T, as follows [35]:

- if $z^* < z^*_T$:
$$T^* = Pr\, z^* \tag{3}$$
- if $z^* > z^*_T$:
$$T^* = Pr_t \left(\frac{1}{\kappa} \times \ln\left(E\, z^*\right) + P \right) \tag{4}$$
with:
$$P = 9.24 \left[\left(\frac{Pr}{Pr_w} \right)^{3/4} - 1 \right] \left[1 + 0.28 e^{-0.007 \frac{Pr}{Pr_{t,w}}} \right] \tag{5}$$

ACCEPTED MANUSCRIPT

z_T^* corresponds to the z^* value at which the linear and logarithmic laws intersect.

Given T^*, either T_w or q_w can be computed depending on the specified boundary condition at walls according to

$$T^* = \frac{(T_w - T_P)\,\rho\,C_P\,C_\mu^{1/4}\,k_p^{1/2}}{q_w} \tag{6}$$

h_w can then be deduced according to Eq.1.

2. Validation of the LRNM model: effect of the turbulence model

2.1. Reference test case and computational model

2.1.1. Experimental configuration

The case study is a wind-tunnel test involving a $H = 1.5\,\text{cm}$ high heated cube placed in a developing boundary layer [12]. This configuration basically addresses more electronic than building physics problems. However, anisotherm experimental data are scarce and this study was also used to validate the LBM LES aerodynamic model addressed by [36, 37][1] as well as the LRNM model of [19].

The test section of the wind-tunnel used is 40 H wide and 3.3 H high. The approach flow has a bulk velocity of $4.47\,\text{m}\cdot\text{s}^{-1}$ and a temperature of 21 °C. The obstacle is composed of an internal copper core uniformly heated at 75 °C covered by a $1.5 \times 10^{-3}\,\text{m}$ thick epoxy layer. The leading face of the cube was located 50 H downwind a trip. Measurements of the external surface temperature were taken using infrared thermography and $h_{c,w}$ was derived from the local heat transfers with an accuracy of 5 to 10 %.

The Reynolds number of the test considered is $Re = 4.4 \times 10^3$ and the Richardson number is $Ri \approx 1.4 \times 10^{-3}$. This is a case of predominant forced convection and buoyancy effects can be neglected.

[1] In complement to wind-tunnel data, this model was used as reference for the validation of the aerodynamic model [6].

ACCEPTED MANUSCRIPT

		epoxy	air	others
ρ	$[\mathrm{kg \cdot m^{-3}}]$	1191	1.225	adiabatic
C_P	$[\mathrm{J \cdot kg^{-1} \cdot K^{-1}}]$	1650	1006.43	
λ	$[\mathrm{W \cdot m^{-1} \cdot K^{-1}}]$	0.237	0.0242	
T	[K]	$T_{w,int} = 348$	$T_{inlet} = 294$	

Table 1: Thermal properties of the model used.

2.1.2. Coupled aerodynamic and thermal model

Due to incomplete information about the experimental setup and as done in Ref. [19], the approach flow profile was firstly designed by modeling a 66 H long, 11 H wide and 3.3 H high empty domain. The approach flow profile was recorded 45 H from the inlet plane, i.e. 5 H upstream the actual location of the cube front face. This profile was set as inlet conditions for the actual simulations, for which only a 5 H long fetch was kept as recommended in Ref. [38, 39]. The epoxy layer was explicitly modeled whereas the copper core was only modeled by an internal wall temperature boundary condition of 75 °C. The inflow temperature was set to 21 °C. The top and bottom boundaries were specified as adiabatic no slip smooth walls. Tab. 1 synthesizes the thermal features of the model.

The cube surfaces were modeled as zero roughness height (smooth) walls. The mesh was refined near the floor and even more next to the fluid/solid interface and within the epoxy layer, down to 3×10^{-4} m. More than 4.4×10^6 cells compose the mesh, including more than 4.8×10^5 cells in the volume of epoxy and 3.9×10^6 tetrahedral cells in the fluid. As such, $z^* \approx 1$ on the cube surface. Simulations were performed using Ansys Fluent 15 [33] using a GPU-based calculation server running Linux. Steady RANS RSM as well as Rk-ε simulations were performed to assess the differences in $h_{c,w}$ predictions due to the turbulence modeling. Compared to eddy viscosity models, the RSM can account for the history and transport of the flow by considering individually each Reynolds stress and can thus account for anisotropic turbu-

ACCEPTED MANUSCRIPT

lence effects. However, the implementation of this model is more demanding than eddy viscosity models and less critical studies and developments are therefore available.

The EWT takes care of near wall regions. Second order numerical schemes were used. Pressure and velocity were coupled using the SIMPLE algorithm and the pressure strain correlation of the RSM was chosen linear. Simulations were initialized with 2×10^3 iterations accounting for standard WFs instead of the EWT to avoid numerical stability problems. The solution iterative convergence was studied by monitoring T_w and $h_{c,w}$ on the vertical and horizontal mid lines of the cube. These profiles were then confronted to the reference experimental data of Meinders et al. [12] and steady RANS Rk-ε numerical data of Defraeye et al. [19].

2.2. Results analysis

Fig. 1 compares the different experimental and numerical profiles of $h_{c,w}$ for the two mid-lines circling the cube. The reported numerical $h_{c,w}$ profiles differ either by the turbulence model used or the number of iterations considered.

A first analysis indicates that the EWT/LRNM approach is reasonnable. Profiles show symmetric behaviors where expected and the order of magnitude of $h_{c,w}$ corresponds to the experimental one. In addition, profiles obtained using the Rk-ε model correspond well to the reference ones, which suggests a good implementation of the model.

Nonetheless, Fig. 1(b) does not show stabilized RSM-$h_{c,w}$ profiles as functions of the number of iterations though simulation was stopped after 9.5×10^3 iterations. This is especially the case on the lateral faces of the cube, where the experiment reports a strong unsteady behavior of the flow. Such a behavior is observable in simulations as the wake fluctuates from one side of the theoretical symmetry plane to the other. In fact, coherent vortex shedding structures develop around isolated cubes, and vorticity shed from the cube lateral faces may induce a yaw of the arch vortex and wake. These processes may prevent the flow to be statistically stationary. Consequently,

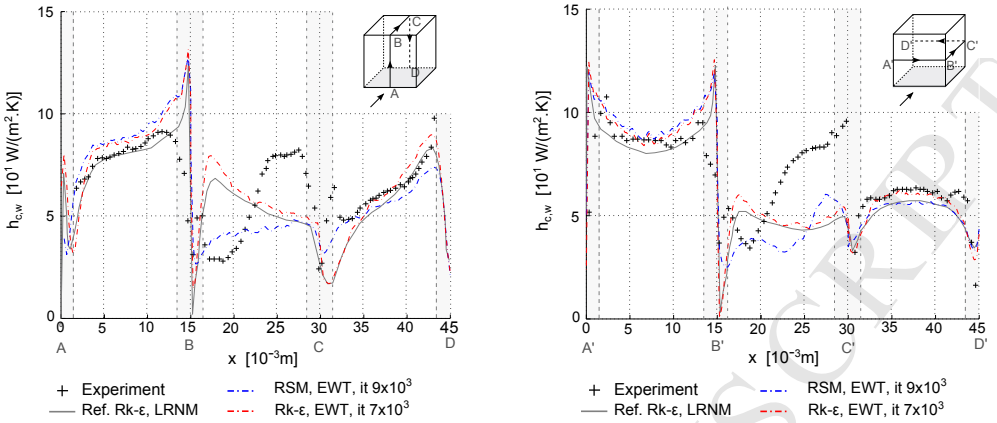

(a) Influence of the turbulence model (steady RANS RSM *vs.* Rk-ε).

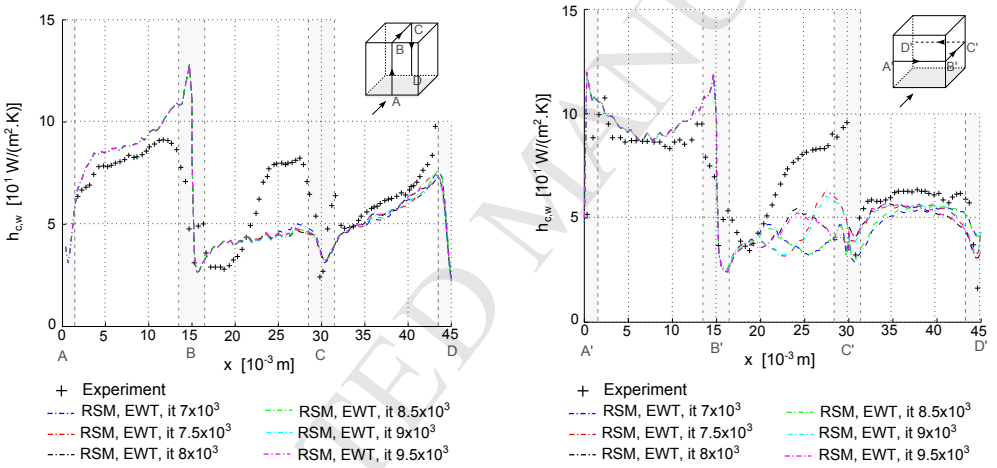

(b) Convergence study for the steady RANS RSM configuration.

Figure 1: Comparison of numerical and experimental $h_{c,w}$ profiles around the cube. Slight grey strips represent regions of higher experimental uncertainties. Experimental data are taken from Ref. [12] and reference (Ref.) R-k-ε LRNM data are taken from [19].

the Reynolds average may not correspond to the time averaging of the solution [40]. Note that such an "unsteady" behavior was also observed for other case studies (see [6]), still where the experimentation stresses strong flow unsteadiness or strong vortex shedding effects. This behavior does not occur when using k-ε models as they are more dissipative. Such observations can

ACCEPTED MANUSCRIPT

call into question the ordinary implementation of steady RANS approaches to study complex flows and the related physical processes developing around constructions.

Nonetheless, beyond the fluctuations that occur during RSM computations, Fig. 1(a) shows a satisfactory match between all the simulated $h_{c,w}$ profiles and the experimental measures for the front face of the cube in terms of distribution and averaged value. A slight over-estimation of $h_{c,w}$ by both steady RANS models is however observed. Larger discrepancies occur next to the top edge, where uncertainties on experimental data are also higher.

The accuracy of numerical predictions is also satisfactory for the rear face of the cube with respect to experimental data, but discrepancies between the predictions obtained using the different turbulence models are no more negligible. RSM predictions of $h_{c,w}$ are less than 10 % lower than those we obtained using the Rk-ε model along the horizontal mid-line, which yields predictions that better correspond to experimental data except near the edges of the face. Focusing on the vertical profile, on the one hand, the slope of the RSM profile corresponds well to the experimental one, but the $h_{c,w}$ intensity is under-estimated by about 8 %, which slightly exceeds the experimental uncertainty. On the other hand, the averaged value of $h_{c,w}$ appears well reproduced by the Rk-ε model, but the slope of the profile is steeper than reported by the experiment.

Contrarily to the front and rear faces, numerical predictions substantially deviate from experimental data on the top and lateral faces, where separated bubbles involving high $h_{c,w}$ gradients with maximum values in reattachment regions and minimum values next to recirculation cores [12]. These recirculation phenomena are generally poorly reproduced by steady RANS models, which certainly explain the deviation observed. Moreover, predictions also differ depending on the turbulence model. As in the experiment, RSM-based $h_{c,w}$ profile increases streamwise on the top face of the cube and a relatively good, but unstabilized, profile shape is even predicted on the cube lateral face. However, $h_{c,w}$ intensities and gradients are under-estimated compared

ACCEPTED MANUSCRIPT

to experimental data. Rk-ε predictions completely differ from experimental data in distribution on the top and lateral faces of the cube. Although a decreasing profile streamwise is simulated on the top face, line averaged $h_{c,w}$ values match the experimental one on the top face.

As a conclusion, both the steady RANS Rk-ε and RSM accurately predicts $h_{c,w}$ profiles on the front and rear faces of the cube when used with the LRNM. However, large deviations between the experimental and numerical profiles, as well as between the predictions obtained using different turbulence models, occur on the other faces, where complex separated flows develop. The RSM seems to predict $h_{c,w}$ distribution better than the Rk-ε does on the top and lateral faces of the cube. Nonetheless, $h_{c,w}$ intensities are under-estimated and the simulated $h_{c,w}$ profiles fluctuate where the flow is physically strongly unsteady.

3. Comparison between LRNM and WFs-based predictions of $h_{c,w}$: effect of the near-wall treatment

3.1. Reference test case and computational model

3.1.1. Reference LRNM study

The case study is a 10 m high cube located in a turbulent boundary layer, which represents a building. WFs are generally required for such a configuration because of the model dimensions. Given the model validation of Sec.2 and literature results showing the better accuracy of fine grid approaches (Sec.1), LRNM data are selected to evaluate predictions obtained using WFs. These LRNM data are provided by Defraeye et al. [41, 19, 25] and were computed using the Rk-εmodel.

As recommended in Ref. [39], the cube is located 5 H from the inlet, lateral and top boundaries of the domain and 15 H from the outlet plane. Lateral boundary conditions were set periodic and the top boundary condition symmetric. A smooth wall boundary condition was specified for the bottom of the domain. An equilibrium ABL profile ($z_0 = 0.03$ m) was specified as inlet condition according to the guideline given in Ref. [39]. Although z_0

ACCEPTED MANUSCRIPT

is small and because of the smooth bottom boundary condition, streamwise gradients necessarily develop along the domain. Nevertheless, this happens for the simulations performed using both the LRNM and WFs so that comparison is done under similar conditions. The reference study was performed for $U_{10} = 0.5\,\mathrm{m}\cdot\mathrm{s}^{-1}$. The inflow and building temperature are 10 °C and 20 °C respectively. This configuration involves $Re > 3\times10^5$ and $Ri = 13.46$, which means that the flow is turbulent and that buoyancy would effectively influence the flow in reality. However, only forced convection processes were considered to save computational resources and keep a reasonable size for near wall cells, yet implementing a LRNM approach. Furthermore, Defraeye et al. [19] showed the relevancy of such an approach to deduce $h_{c,w}-U_{10}$ correlations that are relevant for higher wind speeds.

Two different mesh resolutions that only differ next to walls were used. 2.6×10^6 cells composed the mesh used to perform the LRNM-based simulation ($z^* < 3$ on the cube edges) and 1.1×10^6 cells composed the mesh used to perform the WF-based simulation ($10 \leq z^* \leq 280$ on the cube surfaces).

3.1.2. Computational model

The modeling strategy implemented in the current study is almost similar to that described in Ref. [19], including the domain size, inflow conditions and most of the model settings. Nonetheless, the mesh is unstructured and composed of 2.0×10^6 cells, with 1 m cells on the floor and 0.3 m cells on the cube roof. This implies $z^* \approx 460$ and $z^* \approx 230$ on average on the cube front and rear faces respectively. The top and lateral boundary conditions were set symmetric. Air was modeled as constant density gas (forced convection). Fig. 2 synthesizes the computational model used.

Similarly to Sec. 2, simulations were performed using both the steady RANS RSM and the Rk-ε model. However, standard WFs take care of near wall regions. Convergence was verified by monitoring $h_{c,w}$ profiles on the mid-lines of the different faces of the cube as well as the overall contours of $h_{c,w}$ on these faces.

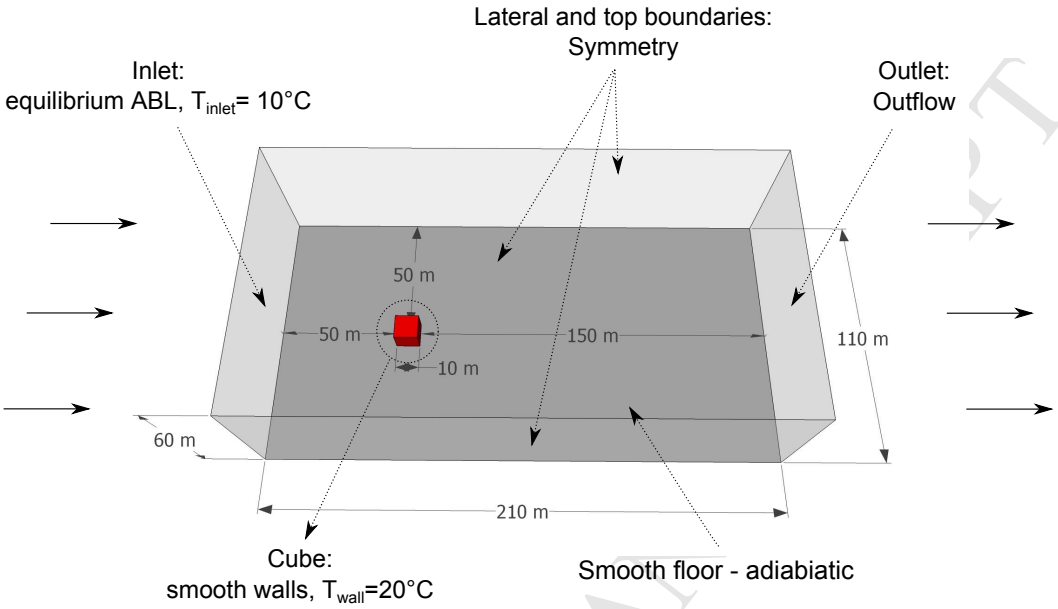

Figure 2: Computational model.

3.2. Results analysis

Fig. 3 compares the simulated $h_{c,w}$ profiles to the reference ones [19] for the horizontal and vertical mid-lines of the cube. Reference results obtained using the LRNM approach or standard WFs are reported in order to distinguish the respective influence of the near wall treatment and the turbulence model. As expected, predictions obtained using the Rk-ε models together with standard WFs correspond to the reference $h_{c,w}$ profiles computed using similar computational settings, which supports a good implementation of the model.

Standard WF significantly over-estimate LRNM data. This observation is supported by literature studies: a substantial over-prediction of $h_{c,w}$ with differences up to 60 % compared to LRNM predictions are highlighted in Ref. [25] and [18]. In addition, $h_{c,w}$ intensities differ depending on the turbulence model used. $h_{c,w}$ intensities predicted by the RSM are lower than those predicted using the Rk-ε model except on the rear face of the cube. RSM

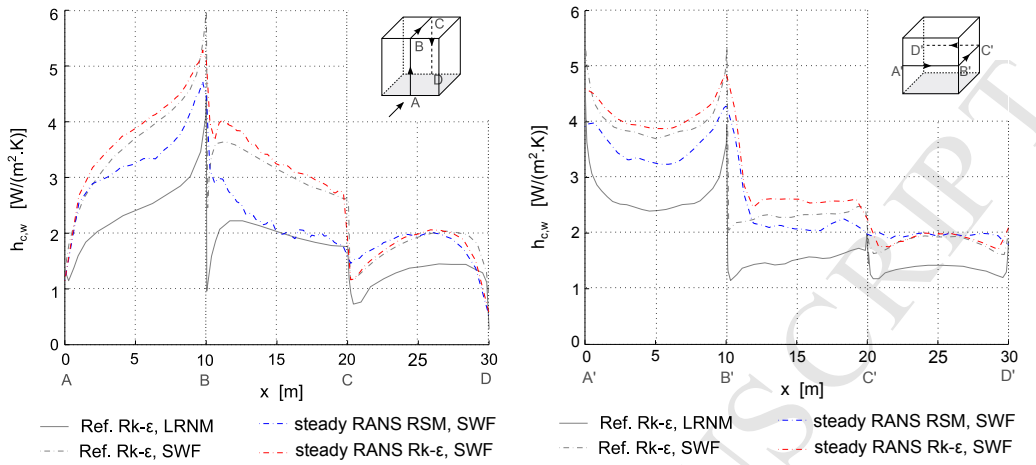

Figure 3: Comparison of the $h_{c,w}$ profiles around the cube: effect of the turbulence model and near-wall treatment. Reference (Ref.) R-k-ε LRNM and SWF data are taken from [25].

predictions over estimate LRNM results by 35 % while deviation is of 60 % with the Rk-ε model. As the shape of $h_{c,w}$ profiles predicted by the two turbulence models are relatively comparable on the different faces of the cube, differences in $h_{c,w}$ intensities may be due to a better estimate of k by the RSM.

As a conclusion, the current study verifies that $h_{c,w}$ profiles predicted by standard WFs significantly deviate from LRNM results. Given the validation study of Sec. 2 and literature results, SWfs may not be considered sufficiently accurate to be generally used for building physics problems even if deviation is reduced when using the steady RANS RSM instead of the Rk-ε model.

4. Design of an adapted temperature wall-function for the RSM based on LRNM data

4.1. Reference customized temperature wall-function

It is possible to improve the accuracy of usual TWFs with respect to LRNM results by modifying the wall turbulent Prandtl number value ($Pr_{t,w}$) both for interior or exterior problems [42, 25]. Focusing on external convective heat transfers, Defraeye et al. [25] proposed a CTWF to be used with

ACCEPTED MANUSCRIPT

the steady RANS Rk-ε model in case of turbulent forced convection, based on the analysis of the $T^* - z^*$ profiles computed using the LRNM. Fig. 4(a) shows that these profiles follow an universal behavior characterized by logarithmic correlations especially for $10^5 < z^* \leq 4 \times 10^3$ at least for wind speeds higher than $0.5\,\mathrm{m} \cdot \mathrm{s}^{-1}$. Fitting this relations using Eq.4 is possible in Fluent by modifying the $Pr_{t,w}$ from 0.85 to 1.95 (see Fig. 4(b)). With this modification, WF-based predictions deviate by less than 10 % with respect to LRNM data instead of 40 % with standard WF in case of an isolated cube and other cuboids representing buildings. This CTWF was also studied for the cubical building immersed in a turbulent boundary layer in case of mixed convection ($0 \leq Ri \leq 52$) [43]. CTWF predictions deviate by less than 16 % compared to LRNM data while the deviation observed with standard wall-functions was of 47 %. Still considering mixed convection cases ($0.14 \leq Ri \leq 13.7$) but a street canyon, the CTWF performs well for mixed convective flows, whereas the standard TWF is more accurate for forced convective flows. As a result, an adaptive TWF was designed to account for both occurrences of flow regimes in a street canyon, by fitting one or the other TWF depending on the local Richardson number [44]. This adaptive TWF generally deviates by less than 10 % compared to LRNM data over the range of Richardson numbers tested.

The different above-mentioned modified TWFs substantially improve the correspondence between WFs wand LRNM predictions. However, their applicability is constrained due to the methodology implemented to determine them as discussed in Ref. [19]. In particular, focusing on forced convection problems, Fig. 4(b) shows that the CTWF would better apply for $5 \times 10^1 \leq z^* \leq 5 \times 10^2$ as the fitting was performed for this range of values, which corresponds to the theoretical range for applicability of WFs.

4.2. Adapatation of temperature wall-functions for the RSM

Results of Sec. 3.2 show rather comparable repartitions but different intensities of $h_{c,w}$ on the cube faces when using the RSM and Rk-ε turbulence models. Moreover, the expression of standard WFs is the same for both

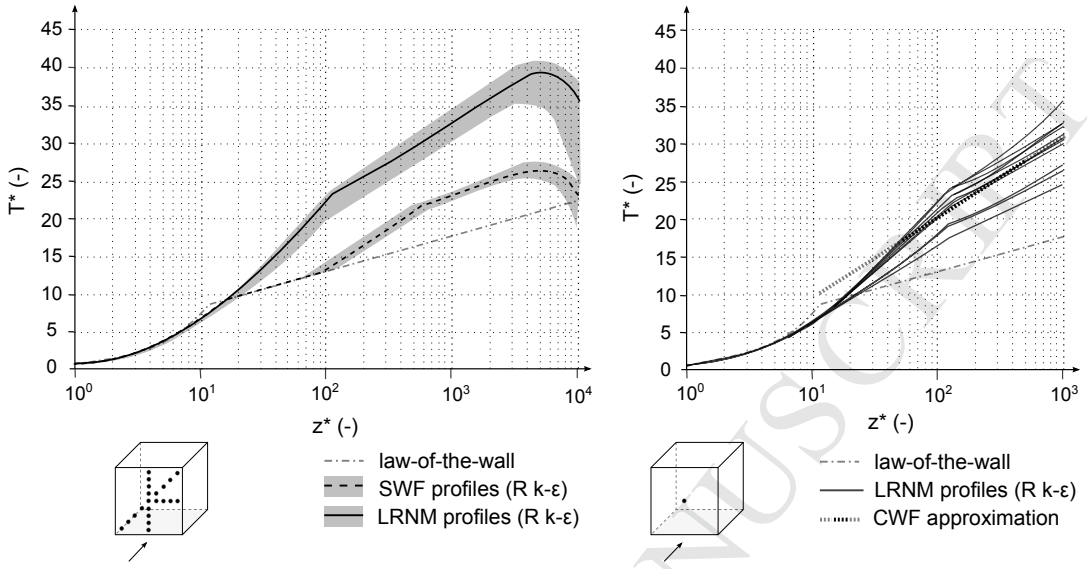

(a) $T^* - z^*$ universal profile [14]. The second log law can be deduced as $T* = 8.87 \ln z^* + 2.5$

(b) Fitting of the R-k-εCTWF for $50 \leq z^* \leq 500$ [25]

Figure 4: Bases of the CTWF.

models. Therefore, a modification of the $Pr_{t,w}$ would also decrease the deviation between the $h_{c,w}$ profiles predicted using WFs and those derived from a LRNM approach when using the RSM. However, T^* being a function of k, results may differ depending upon the turbulence model used. Its reliability when used together with other turbulence models deserves further research.

Fig. 5 compares the $h_{c,w}$ profiles we obtained accounting for $Pr_{t,w} = 1.95$ together with either the steady RANS RSM or the Rk-ε model to the reference LRNM and CTWF $h_{c,w}$ profiles from Ref. [25]. The two mid lines circling the 10 m high cubic building are still addressed. Results show a good match between our steady RANS Rk-ε-CTWF results and the reference profiles. However, $h_{c,w}$ profiles simulated by the RSM under-estimate LRNM results by 20 % and 25 % on average on the front and top faces of the cube. $h_{c,w}$ is also under-estimated on the lateral face, and its distribution is predicted more constant compared to LRNM data. As this behavior occurs also when using the Rk-ε model, it may be explained by WF effects rather than

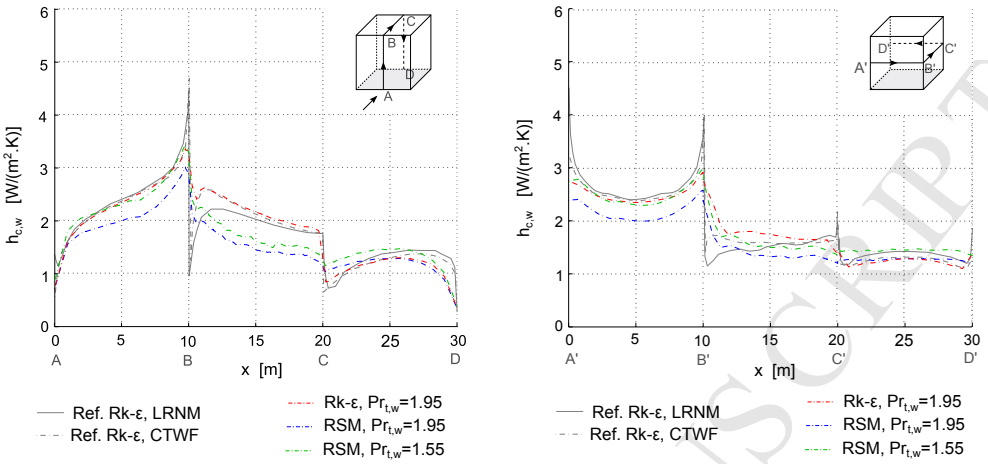

Figure 5: Comparison of the h profiles obtained using customized $Pr_{t,w}$ values with reference (Ref.) R-k-ε LRNM data [41].

turbulence model effects.

According to Eq. 6 and Eq. 4, $q_{w,c}$, and likewise $h_{c,w}$, is a decreasing function of $Pr_{t,w}$. Therefore, different $Pr_{t,w}$ values lower than 1.95 were tested to fit LRNM results when using WFs and the RSM. Fig.5 shows a good match between simulations outputs and LRNM $h_{c,w}$ profiles for $Pr_{t,w} = 1.55$, with a correspondence comparable to that of the Rk-ε-CTWF.

To further verify the accuracy of the RSM-CTWFs ($Pr_{t,w} = 1.55$), several simulated $h_{c,w}$ profiles were compared to the LRNM predictions of Defraeye [41][2] for different vertical lines on the front and rear faces of the cube, i.e. where LRNM data are validated (Sec. 2). As the problem is symmetric, Fig. 6 reports the results obtained using both turbulence models and the appropriate $Pr_{t,w}$ value for three vertical profiles located 1 m and 3 m from the edge and on the symmetry axis of the faces.

Not considering border locations, customized TWF-based $h_{c,w}$ profiles match very well with each other and with LRNM results on the front face of the cube. However, the simulated $h_{c,w}$ profiles deviate from each other

[2]These LRNM-based $h_{c,w}$ profiles were kindly provided to us by T. Defraeye.

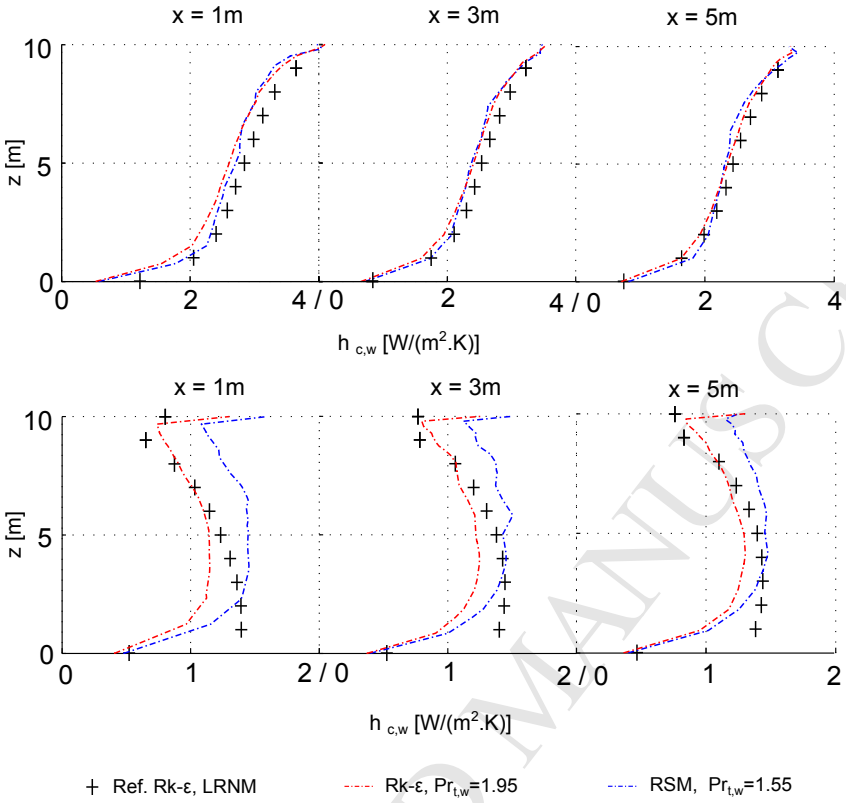

Figure 6: Comparison between the simulated h profiles using the R-k-ε model with $Pr_{t,w} = 1.95$ or the RSM - CTWF with $Pr_{t,w} = 1.55$ with reference LRNM [41] on the front (top) and rear (bottom) faces of the cubical building and for $U_{10} = 0.5\,\mathrm{m}\cdot\mathrm{s}^{-1}$.

and from LRNM results on the rear face. RSM predictions deviate by up to 20 % at mid height, which is not negligible, but is much less than the 70 % observed in Fig. 3 for standard WFs. Hence, accounting for the RSM-CTWF instead of standard WFs gives satisfactory results on the front and rear faces of cubical buildings with respect to LRNM data.

4.3. Pertinence of the RSM customized temperature wall-function for high z^*

Assuming cell sizes of about 0.5 m, the CTWFs relevantly apply for relatively low wind speeds ($50 \leq z^* \leq 500$). Considering the case study of Sec. 3, increasing the reference wind speed from e.g. $U_{10} = 0.5\,\mathrm{m}\cdot\mathrm{s}^{-1}$ to

	Front face				Rear face			
U_{10}	$0.5\,\mathrm{m\cdot s^{-1}}$		$5\,\mathrm{m\cdot s^{-1}}$		$0.5\,\mathrm{m\cdot s^{-1}}$		$5\,\mathrm{m\cdot s^{-1}}$	
$h_{c,w}-U_{10}$	2.78		19.68		1.28		8.63	
	$h_{c,w}$	d.(%)	$h_{c,w}$	d.(%)	$h_{c,w}$	d.(%)	$h_{c,w}$	d.(%)
Rk-ε, SWF	4.0	43.9	–		– 1.6	27.3	–	–
Rk-ε, CWF	2.4	12.2	17.8	9.7	1.1	16.4	7.5	12.6
RSM, SWF	3.5	24.8	27.3	38.8	1.7	35.9	13.7	58.5
RSM, CWF	2.5	11	18.4	6.7	1.3	1	9.4	9.2
RSM, CWF M+	–	–	18.6	5.5	–	–	9.8	13.7

Table 2: Comparison of the surface averaged $h_{c,w}$ $[\mathrm{W\cdot m^{-2}\cdot K^{-1}}]$computed using the reference $h_{c,w}-U_{10}$ correlation of [19] or estimated using CFD simulations for the cube in cases of $U_{10}=0.5\,\mathrm{m\cdot s^{-1}}$ and $U_{10}=5\,\mathrm{m\cdot s^{-1}}$. –: Simulation not performed.

$U_{10}=5\,\mathrm{m\cdot s^{-1}}$ does not change the repartition of z^* on the cube front and rear faces but the surface averaged z^* equals 4.6×10^3 on the front face. This z^* value exceeds the usual range for applicability of WFs and CTWFs, although Ref. [25] suggest that the latter may also be relevant for high z^*.

To evaluate the applicability of both the Rk-ε and RSM-CTWFs, additional simulations were performed for the 10 m high cubical building considering $U_{10}=5\,\mathrm{m\cdot s^{-1}}$. This modification does not alter the distributions of $h_{c,w}$ on the cube faces but multiplies the surface averaged $h_{c,w}$ values by a factor 7.3. In such a configuration, $R\geq3\times10^6$ and $Ri\approx0.13$, which means that the flow is turbulent and in predominant forced convection regime.

Considering $U_{10}=0.5$ or $5\,\mathrm{m\cdot s^{-1}}$, Tab. 2 compares surface averaged $h_{c,w}$ intensities estimated using the $h_{c,w}-U_{10}$ correlation of Defraeye et al. [19] or simulated using the Rk-ε and the RSM together with either the standard or the CTWFs. The reference correlation is based on LRNM data ans is formulated as follows [19]:

$$h_{c;w}=5.01\times U_{10}^{0.85} \tag{7}$$

Accordingly to literature results and the observations reported in Sec. 3,

ACCEPTED MANUSCRIPT

the use of standard TWFs significantly over-estimates reference $h_{c,w}$ values. Considering the RSM simulations, the relative deviation is more than a factor 1.5 greater in case of $U_{10} = 5\,\mathrm{m \cdot s^{-1}}$ than in case of $U_{10} = 0.5\,\mathrm{m \cdot s^{-1}}$, and reaches nearly 60 % on the rear face. On the contrary, the accuracy of CTWFs is generally improved in case of $U_{10} = 5\,\mathrm{m \cdot s^{-1}}$ except on the rear face of the cube when using the RSM. However, the deviation is smaller than 10 % in comparison with the reference data, which remains acceptable considering the uncertainties linked with steady RANS and usual building physics models. Still considering $U_{10} = 5\,\mathrm{m \cdot s^{-1}}$, refining the mesh improves the accuracy of the RSM-CTWF predictions on the front face of the cube, but reduces it on the rear face. Nevertheless, the loss of accuracy is of $0.38\,\mathrm{W \cdot m^{-2} \cdot K^{-1}}$ (4.5 points), which is negligible for building physics applications.

Fig. 7 compares CTWF $h_{c,w}$ profiles for the same vertical profiles as in Fig. 6 with LRNM data [41], but considers $U_{10} = 5\,\mathrm{m \cdot s^{-1}}$. Results show a very good match between LRNM and CTWF -based $h_{c,w}$ profiles on both faces when using the Rk-ε model. RSM-CTWF results match LRNM data on the front face but over-estimates them on the rear face. As expected from Tab. 2, a loss of accuracy of these predictions occurs compared to the configuration with $U_{10} = 0.5\,\mathrm{m \cdot s^{-1}}$. Deviation decreases towards the symmetry axis. Predictions typically deviate from LRNM results by 30 % and 15 % 1 m from the lateral edge of the face and on the symmetry axis respectively. Nevertheless, Sec. 2 shows that the RSM predicts more constant horizontal profiles of $h_{c,w}$ on the rear face of the obstacles than the Rk-ε does, which better corresponds to experimental data. As a consequence, the deviation observed between the RSM-based profiles and the reference Rk-ε LRNM data may be not only due to the TWF used, but also (and even mainly) to the turbulence model.

Hence, Rk-ε and the RSM-CTWFs appear accurate both in terms of distribution and intensity on the front face of the cube for high z^* values. Contrarily to Rk-ε results, RSM results deviate from Rk-ε/LRNM predictions on the rear face. Nevertheless, the predicted surface averaged $h_{c,w}$ values are

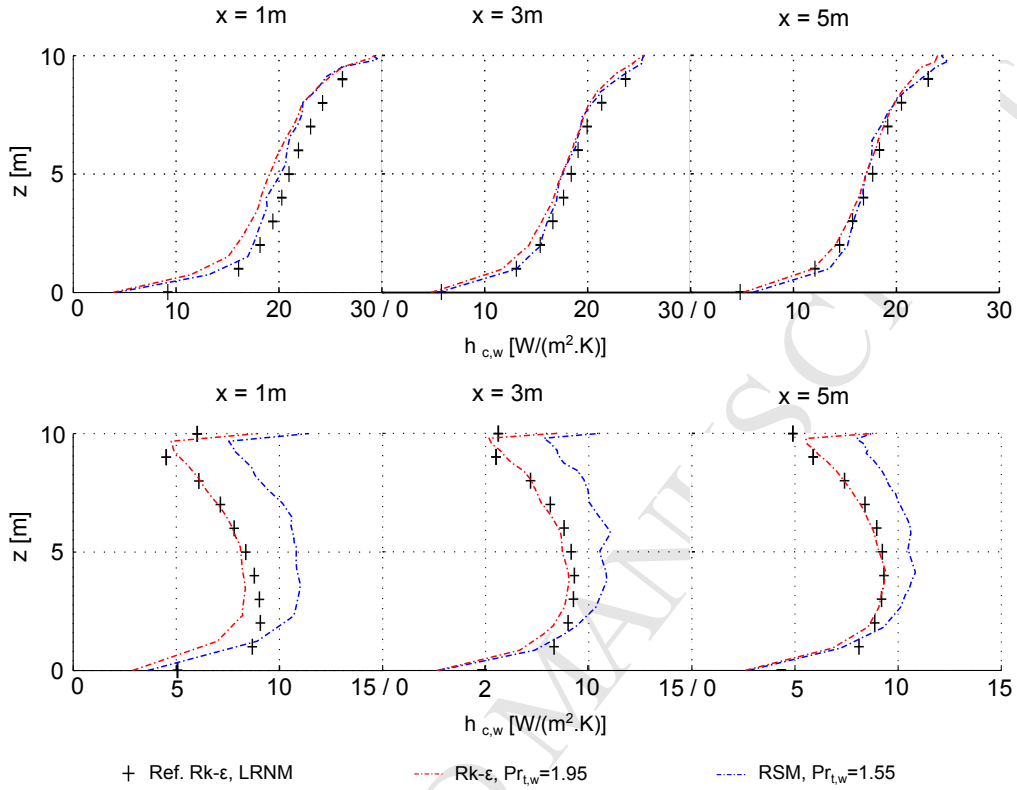

Figure 7: Comparison between the simulated h profiles using the R-k-ε or RSM - CTWF with reference LRNM data [41] on the front (top) and rear (bottom) faces of the cubical building and for $U_{10} = 5\,\mathrm{m}\cdot\mathrm{s}^{-1}$.

satisfactory, and the accuracy of predictions is significantly improved with respect to LRNM data compared to that obtained using standard TWFs.

5. Discussion and outlooks

Because CFD models can account for any built environment, they are valuable to provide estimates of $h_{c,w}$ suitable for use in building physics. However, their accuracy is very dependent on the CFD method used. Although real atmospheric flows are generally not statistically stationary, steady RANS models are mostly used in environmental wind and building energy engineer-

ACCEPTED MANUSCRIPT

ing because other methods are still too computationally expensive. As a consequence, the accuracy of the turbulence models used is of challenging concern as it determines the physical accuracy of the computed flow field as well as convective heat transfer predictions (Sec. 2). In particular, second order turbulence models may perform better than usual two equation models in predicting complex flows, where turbulence anisotropy is important [3, 45, 6].

In addition to the effects of the turbulence model, the determination of $h_{c,w}$ at building outer walls is very dependent on the near wall treatment. Standard WF substantially devaite from LRNM data for complex separated flows around constructions (Sec. 3). Nonetheless, although being more accurate, performing LRNM simulations is rarely possible, still because of the computational costs involved. Therefore, improved TWFs were developed, but they mainly address k-ε models [25, 44].

Extending the studies reported in Ref. [19] and [25], the RSM-CTWF developed in Sec. 4.2 aims at enlarging the scope for applicability of CTWF to more detailed turbulence models. Due to the implemented design methodology, this RSM-CTWF has almost the same advantages, drawbacks and scope of applicability as the Rk-ε-CTWF proposed in Ref. [25] though the applicability of both CTWFs was studied for high z^*. In particular, its use is relevant for forced convection problems and the front (and rear faces) of an isolated sharp edged building.

Further than simply highlighting differences between predictions obtained using the Rk-ε or the RSM models, the LRNM or WFs and proposing a version of the CTWF suitable for use with the RSM, the current study also arises other substantial modeling challenges. Essentially, intermittent convective processes are identified as a significant issue for steady RANS methods, as they greatly impacts of convective heat transfers. Because of their transient formulation, unsteady RANS approaches and even more large eddy simulation (LES) methods should improve the physical accuracy of simulations [31, 46, 47].

ACCEPTED MANUSCRIPT

Moreover, this study only considers one wind direction, forced convection and isolated sharp edged obstacles with smooth walls. To come closer to real building physics problems, further studies should extend the approach to more realistic environments by considering different wind directions and speeds [48], buoyancy effects [14, 44], multi-obstacles configurations [49] and wall roughness effects [50]. Furthermore, this approach might advantageously be extended to lower z^* by blending a near wall model for viscosity affected regions, which would be useful when automatic grid generation algorithms place first nodes in such regions [30]. This approach might also advantageously be integrated in a coupling between CFD and building energy models to reciprocally provide appropriate boundary conditions as it has been done for the interior of buildings [51, 1, 2], thus improving our understanding of the interactions between the building and its environment.

Conclusion

This paper firstly examined the accuracy of the steady RANS methods and RSM and Rk-ε turbulence models in predicting convective heat transfers around a sharp edged obstacle by performing a LRNM approach. Steady RANS approaches show difficulties to predict convective heat transfers in complex and unsteady separated flows and the predicted $h_{c,w}$ distribution deviates depending on the turbulence model used. Nonetheless, both turbulence models provide accurate $h_{c,w}$ estimates on the front and rear face of the isolated obstacle. Switching to a more realistic - but still theoretical - building model, it is verified that standard TWF substantially over-predicts convective heat transfers at building outer walls compared to LRNM results either when used with the Rk-ε or the RSM. Assuming LRNM results accurate given the validation study and literature findings, and given the necessity of using WFs in building physics CFD simulations, this study aimed to provide a TWF able to reproduce LRNM results for the RSM. This model may be more accurate than eddy viscosity models in complex configurations. Based on suggestions of Ref. [25], a calibration of the $Pr_{t,w}$ was done. The

ACCEPTED MANUSCRIPT

RSM-CTWF implies to modify the $Pr_{t,w}$ in Ansys Fluent to 1.55 instead of 0.85 by default in the software [33] and 1.95 for the Rk-ε-CTWF [25].

To conclude, the use of CTWFs together with the appropriate turbulence model substantially improves $h_{c,w}$ predictions as compared to standard TWF on the front and rear faces of isolated sharp-edged obstacles lying perpendicular to the wind at least. Nonetheless, to even more improve the accuracy of $h_{c,w}$ estimates, a more detailed CFD approach should be used. Indeed accurately modeling convective heat transfers implies modeling more accurately the aerodynamic field in terms of dynamic features as well as the near wall region. Therefore, methods such as the cost effective LBM LES [37] appear promising as they allow a detailed computation of the different scales of the flow field on a very fine spatial an temporal discretization.

Acknowledgments

Authors thanks T. Defraeye for providing the useful reference LRNM data.

References

[1] Z. J. Zhai, Q. Y. Chen, Performance of coupled building energy and CFD simulations, Energy and Buildings 37 (4) (2005) 333–344.

[2] Z. J. Zhai, Q. Y. Chen, Sensitivity analysis and application guides for integrated building energy and CFD simulation, Energy and Buildings 38 (9) (2006) 1060–1068.

[3] M. G. Emmel, M. O. Abadie, N. Mendes, New external convective heat transfer coefficient correlations for isolated low-rise buildings, Energy and Buildings 39 (3) (2007) 335–342.

[4] J. Bouyer, C. Inard, M. Musy, Microclimatic coupling as a solution to improve building energy simulation in an urban context, Energy and Buildings 43 (7) (2011) 1549–1559.

ACCEPTED MANUSCRIPT

[5] J. Allegrini, V. Dorer, J. Carmeliet, Analysis of convective heat transfer at building facades in street canyons and its influence on the predictions of space cooling demand in buildings, Journal of Wind Engineering and Industrial Aerodynamics 104-106 (2012) 464–473.

[6] L. Merlier, On the interactions between urban structures and air flows: a numerical study of the effects of urban morphology on the building wind environment and the related building energy loads, Ph.D. thesis, INSA de Lyon, Lyon, France (2015).

[7] J. Palyvos, A survey of wind convection coefficient correlations for building envelope energy systems modeling, Applied Thermal Engineering 28 (8-9) (2008) 801–808.

[8] S. Saneinejad, P. Moonen, T. Defraeye, J. Carmeliet, Analysis of convective heat and mass transfer at the vertical walls of a street canyon, Journal of Wind Engineering and Industrial Aerodynamics 99 (4) (2011) 424 – 433.

[9] T. Oke, Boundary layer climates, 2nd Edition, Routedge, 1987.

[10] J. Allegrini, V. Dorer, J. Carmeliet, Influence of morphologies on the microclimate in urban neighbourhoods, Journal of Wind Engineering and Industrial Aerodynamics 144 (2015) 108–117.

[11] R. Cole, N. Sturrock, The convective heat exchange at the external surface of buildings, Building and Environment 12 (1977) 207–214.

[12] E. Meinders, K. Hanjalic, R. Martinuzzi, Experimental study of the local convection heat transfer from a wall mounted cube in turbulent channel flow, Journal of heat transfer 121 (1999) 564–573.

[13] H. Nakamura, T. Igarashi, T. Tsutsui, Local heat transfer around a wall-mounted cube in the turbulent boundary layer, International Journal of Heat and Mass Transfer 44 (2001) 3385–3395.

ACCEPTED MANUSCRIPT

[14] T. Defraeye, B. Blocken, J. Carmeliet, Convective heat transfer coefficients for exterior building surfaces: Existing correlations and CFD modelling, Energy Conversion and Management 52 (1) (2011) 512–522.

[15] H. Nakamura, T. Igarashi, T. Tsutsui, Local heat transfer around a wall-mounted cube at 45 to flow in a turbulent boundary layer, International Journal of Heat and Fluid Flow 24 (6) (2003) 807–815.

[16] A. Hagishima, J. Tanimoto, Field measurements for estimating the convective heat transfer coefficient at building surfaces, Building and Environment 38 (7) (2003) 873–881.

[17] Y. Liu, D. Harris, Full-scale measurements of convective coefficient on external surface of a low-rise building in sheltered conditions, Building and Environment 42 (7) (2007) 2718–2736.

[18] B. Blocken, T. Defraeye, D. Derome, J. Carmeliet, High-resolution CFD simulations for forced convective heat transfer coefficients at the facade of a low-rise building, Building and Environment 44 (12) (2009) 2396–2412.

[19] T. Defraeye, B. Blocken, J. Carmeliet, CFD analysis of convective heat transfer at the surfaces of a cube immersed in a turbulent boundary layer, International Journal of Heat and Mass Transfer 53 (1-3) (2010) 297–308.

[20] M. Mirsadeghi, D. Cstola, B. Blocken, J. Hensen, Review of external convective heat transfer coefficient models in building energy simulation programs: Implementation and uncertainty, Applied Thermal Engineering 56 (1-2) (2013) 134–151.

[21] P. Moonen, T. Defraeye, V. Dorer, B. Blocken, J. Carmeliet, Urban Physics: Effect of the micro-climate on comfort, health and energy demand, Frontiers of Architectural Research 1 (3) (2012) 197–228.

ACCEPTED MANUSCRIPT

[22] B. Blocken, 50 years of Computational Wind Engineering: Past, present and future, Journal of Wind Engineering and Industrial Aerodynamics 129 (2014) 69–102.

[23] B. Launder, Numerical computation of convective heat transfer in complex turbulent flows: time to abandon wall functions?, International Journal of Heat and Mass Transfer 27 (9) (1984) 1485–1491.

[24] B. Launder, On the Computation of Convective Heat Transfer in Complex Turbulent Flows, Journal of heat transfer 110 (4b) (1988) 1112–1128.

[25] T. Defraeye, B. Blocken, J. Carmeliet, An adjusted temperature wall function for turbulent forced convective heat transfer for bluff bodies in the atmospheric boundary layer, Building and Environment 46 (11) (2011) 2130–2141.

[26] L. Merlier, C. Obrecht, F. Kuznik, G. Rusaoun, J. Hans, On the accuracy of steady RANS models and the LBM LES method: Comparison of the predicted flows around an isolated rectangular block, Submitted.

[27] M. I. of Hamburg, Compilation of experimental data for validation of microscale dispersion models (2013).
URL `http://www.mi.uni-hamburg.de/CEDVAL`

[28] B. Leitl, Validation data for microscale dispersion modeling, EUROTRAC Newsletter (22) (2000) 28–32.

[29] B. Blocken, Sports and buildings aerodynamics (MOOC) (Jun. 2014).
URL `Coursera.org`

[30] M. Popovac, K. Hanjalic, Compound Wall Treatment for RANS Computation of Complex Turbulent Flows and Heat Transfer, Flow, Turbulence and Combustion 78 (2) (2007) 177–202.

ACCEPTED MANUSCRIPT

[31] W. Rodi, Comparison of LES and RANS calculations of the flow around bluff bodies, Journal of Wind Engineering and Industrial Aerodynamics 69-71 (1997) 55–75.

[32] X. Albets-Chico, C. Prez-Segarra, A. Oliva, J. Bredberg, Analysis of wall-function approaches using two-equation turbulence models, International Journal of Heat and Mass Transfer 51 (19-20) (2008) 4940–4957.

[33] Fluent inc., Fluent release 14.5 user guide (2013).

[34] M. Wolfshtein, The velocity and temperature distribution in one dimensional flow with turbulence augmentation and pressure gradient, International journal of heat and mass transfers 12 (1969) 301–319.

[35] Fluent inc., Fluent release 14.5 theory guide (2013).

[36] C. Obrecht, F. Kuznik, J.-J. Roux, B. Tourancheau, Toward urban scale flow simulations using the lattice boltzmann method, in: Proceedings of Building Simulation Conference, IBPSA, 2011, pp. 933–940.

[37] C. Obrecht, F. Kuznik, L. Merlier, J.-J. Roux, B. Tourancheau, Towards aeraulic simulations at urban scale using the lattice Boltzmann method, Environmental Fluid Mechanics 15 (4) (2015) 753–770.

[38] J. Franke, Recommendations of the COST action C14 on the use of CFD in predicting pedestrian wind environment, in: The fourth international symposium on computational wind engineering, Yokahoma, Japan, 2006, pp. 529–532.

[39] Y. Tominaga, A. Mochida, R. Yoshie, H. Kataoka, T. Nozu, M. Yoshikawa, T. Shirasawa, AIJ guidelines for practical applications of CFD to pedestrian wind environment around buildings, Journal of Wind Engineering and Industrial Aerodynamics 96 (10-11) (2008) 1749–1761.

ACCEPTED MANUSCRIPT

[40] G. Iaccarino, A. Ooi, P. Durbin, M. Behnia, Reynolds averaged simulation of unsteady separated flow, International Journal of Heat and Fluid Flow 24 (2) (2003) 147–156.

[41] T. Defraeye, LRNM profiles on the front and rear faces of a 10 m high cibical building - unpublished data (2009).

[42] T. T. Zhang, H. Zhou, S. Wang, An adjustment to the standard temperature wall function for CFD modeling of indoor convective heat transfer, Building and Environment 68 (2013) 159–169.

[43] T. Defraeye, B. Blocken, J. Carmeliet, CFD simulation of heat transfer at surfaces of bluff bodies in turbulent boundary layers: Evaluation of a forced-convective temperature wall function for mixed convection, Journal of Wind Engineering and Industrial Aerodynamics 104-106 (2012) 439–446.

[44] J. Allegrini, V. Dorer, T. Defraeye, J. Carmeliet, An adaptive temperature wall function for mixed convective flows at exterior surfaces of buildings in street canyons, Building and Environment 49 (2012) 55–66.

[45] I. Panagiotou, M. K.-A. Neophytou, D. Hamlyn, R. E. Britter, City breathability as quantified by the exchange velocity and its spatial variation in real inhomogeneous urban geometries: An example from central London urban area, Science of the Total Environment 442 (2013) 466–477.

[46] Y. Tominaga, A. Mochida, S. Murakami, S. Sawaki, Comparison of various revised k eps models and LES applied to flow around a high rise building model with 1:1:2 shape placed wityhin the surface boundary layer, Journal of Wind Engineering and Industrial Aerodynamics 96 (2004) 389–411.

[47] P. Moonen, V. Dorer, J. Carmeliet, Evaluation of the ventilation potential of courtyards and urban street canyons using RANS and LES,

ACCEPTED MANUSCRIPT

Journal of Wind Engineering and Industrial Aerodynamics 99 (4) (2011) 414–423.

[48] T. Defraeye, J. Carmeliet, A methodology to assess the influence of local wind conditions and building orientation on the convective heat transfer at building surfaces, Environmental Modelling & Software 25 (12) (2010) 1813–1824.

[49] J. Liu, M. Heidarinejad, S. Gracik, J. Srebric, The impact of exterior surface convective heat transfer coefficients on the building energy consumption in urban neighborhoods with different plan area densities, Energy and Buildings.

[50] K. Suga, T. Craft, H. Iacovides, An analytical wall-function for turbulent flows and heat transfer over rough walls, International Journal of Heat and Fluid Flow 27 (5) (2006) 852–866.

[51] Z. Zhai, Q. (Yan) Chen, Numerical determination and treatment of convective heat transfer coefficient in the coupled building energy and CFD simulation, Building and Environment 39 (8) (2004) 1001–1009.

ACCEPTED MANUSCRIPT